

Article

Estimating the Buckling Load of Steel Plates with Center Cut-Outs by ANN, GEP and EPR Techniques

Jagan Jayabalan ¹, Manju Dominic ², Ahmed M. Ebid ^{3,*}, Atefeh Soleymani ⁴, Kennedy C. Onyelowe ⁵
and Hashem Jahangir ⁶

- ¹ Department of Civil Engineering, Galgotias University, Greater Noida 203201, India
² Department of Civil Engineering, Rajadhani Institute of Engineering and Technology, Thiruvananthapuram 695102, India
³ Department of Structural Engineering, Future University in Egypt, New Cairo 11865, Egypt
⁴ Department of Structural Engineering, Shahid Bahonar University of Kerman, Kerman 76169-14111, Iran
⁵ Department of Civil Engineering, Michael Okpara University of Agriculture, Umudike 440101, Nigeria
⁶ Department of Civil Engineering, University of Birjand, Birjand 97174-31349, Iran
* Correspondence: ahmed.abdelkhaleq@fue.edu.eg

Abstract: Steel plates are used in the construction of various structures in civil engineering, aerospace, and shipbuilding. One of the main failure modes of plate members is buckling. Openings are provided in plates to accommodate various additional facilities and make the structure more serviceable. The present study examined the critical buckling load of rectangular steel plates with centrally placed circular openings and different support conditions. Various datasets were compiled from the literature and integrated into artificial intelligence techniques like Gene Expression Programming (GEP), Artificial Neural Network (ANN) and Evolutionary Polynomial Regression (EPR) to predict the critical buckling loads of the steel plates. The comparison of the developed models was conducted by determining various statistical parameters. The assessment revealed that the ANN model, with an R^2 of 98.6% with an average error of 10.4%, outperformed the other two models showing its superiority in terms of better precision and less error. Thus, artificial intelligence techniques can be adopted as a successful technique for the prediction of the buckling load, and it is a sustainable method that can be used to solve practical problems encountered in the field of civil engineering, especially in steel structures.

Keywords: cut-outs; buckling load; artificial intelligence; steel plates; axial loading



Citation: Jayabalan, J.; Dominic, M.; Ebid, A.M.; Soleymani, A.; Onyelowe, K.C.; Jahangir, H. Estimating the Buckling Load of Steel Plates with Center Cut-Outs by ANN, GEP and EPR Techniques. *Designs* **2022**, *6*, 84. <https://doi.org/10.3390/designs6050084>

Academic Editor: Farshid Aram

Received: 26 August 2022

Accepted: 19 September 2022

Published: 22 September 2022

Publisher's Note: MDPI stays neutral with regard to jurisdictional claims in published maps and institutional affiliations.



Copyright: © 2022 by the authors. Licensee MDPI, Basel, Switzerland. This article is an open access article distributed under the terms and conditions of the Creative Commons Attribution (CC BY) license (<https://creativecommons.org/licenses/by/4.0/>).

1. Introduction

1.1. Background

Plate buckling analysis has a wide range of applications in a variety of engineering domains, such as civil and structural engineering, mechanical engineering, marine, aerospace engineering, etc. [1], particularly when a lightweight design is the main objective [2]. Plate buckling is a type of destabilization that occurs when a sudden deflection occurs under compressive load. Plates buckle when exposed to compressive stresses greater than the critical limit [3,4]. A critical level of stress develops whenever the plates are subjected to compressive load, causing this to occur. The origin of plate buckling is governed by partial differential equations, which makes the interpretation exceedingly difficult [5,6]. A plate with cut-outs has a more sophisticated buckling analysis than a plate without cut-outs [7]. Cut-outs in box girders and certain load-bearing spars save material, can be used as windows or doors, or simply improve the design aesthetics. They also provide ventilation, accessibility for maintenance, installation, and damage assessment. As a result, an in-depth understanding of perforated and non-perforated plate buckling is necessary [8–13]. Perforated plates have lower structural strength than plates without

holes, and buckling behavior is one of the most significant failures to be considered in these systems' safe and reliable operation.

1.2. Literature Review

The existence of cut-outs of varied sizes results in the formation of free edges in steel plates, which causes high stresses, resulting in plate stiffness degradation and early fracture [14–16]. Therefore, for effective design, it is critical for the design engineer to comprehend the stability, overall strength, and failure parameters of steel plates with cut-outs of varied shapes and sizes. A full grasp of buckling stresses and corresponding mode shapes is the cornerstone of dependable structural designs and constructing a straightforward technique can give an acceptable method. Because of the issue's difficulty, most academics investigated the buckling performance of rectangular sheets with perforations and isotropic support using the FEM or Rayleigh-Ritz techniques [17–20].

Numerical, experimental, and analytical methods and their combinations have been used in several important investigations. The impact of a rectangular cut-out on a plate was studied by Suneel Kumar et al. [21]. Several cut-out dimensions, slenderness ratios, and area ratios were employed to get the required result. The impact of changing different factors on the ultimate strength of a plate subjected to axial compression was determined. Ansys simulation was used to verify the findings. The consequences of perforations on the buckling behavior of plates in a linear manner were investigated by Maiorana et al. [22]. Under compressive stresses, the boundary condition completely supported all edges, and circular and square holes were studied. The findings were reported on graphs for circular and square perforations with variations in the position of the cut-outs. Sandeep Singh et al. [23] investigated the effect of partial edge compression, modification in aspect ratio, and the effects of cut-outs on buckling load, discovering that partial edge compression had a larger effect on buckling strength than uniform edge compressive load, and panels without holes had a greater critical load than panels with perforation. Although the effect of partial edge compression on buckling load was less clear. Dadrasi [24] investigated the buckling performance of punctured steel plates with rectangular shapes when subjected to uniaxial compressive stress. Cut-outs in a circle or square were utilized in a variety of loading bands, numeral, and empirical findings. For finite element analysis, ABAQUS software was employed, and for an experimental study, a group of servo-hydraulic INSTRON8802 was utilized. The findings for plates with or without cut-outs were inspected. They found that the critical buckling load ascended as the loading band broadened and, furthermore, that the buckling load for plates with a circular cut-out was higher than for plates with square cut-outs. Djelosevic et al. [25] investigated the elastic stability of panels with varied perforation geometry. For circular, square, and rectangular apertures, several variables' influence on the plate's elastic stability, such as opening form, size, and direction, was investigated, and a sensitivity factor was constructed. The presence of holes, they found, decreased the deformation energy. Whenever thin rectangular plates with cut-outs in the shape of a circle were uniaxially loaded, instability arose far before the yield point, and it occurred prior to the yield point of the panel material when the plates were thick, according to Mauro et al. [26]. The effect of change in plate thickness with a hole regarding plate buckling was investigated by Mohamazadeh and Noh [27]. The buckling coefficient and buckling stresses were determined using the Gerard and Becker formulas. They compared plates with cut-outs against plates without perforations and discovered that if there was an increase in the thickness of the plate, the buckling load and stress also increased. They [28] also examined the effect of perforations on the buckling of thin plates. ABAQUS was used to perform the simulations, and critical values for buckling load and corresponding stress were computed for variations in hole diameter and plate thickness. Shariati et al. [29] studied the buckling behavior of a panel in the shape of a rectangle with a circular hole at various points on the panel under various boundary circumstances, and found that the boundary circumstances had a substantial effect on the buckling behavior. For different aspect ratios, Jana [30] investigated the buckling performance of a rectangular sheet composed of a simple

support border for uniform axial compressive loads with a circular cut-out. For changes in perforation size, aspect ratio, and thickness of the plate, eigenvalue buckling analysis was performed. Using Ansys and MATLAB, he discovered that the ideal perforation location for the highest buckling load is in the middle of the axis on which the stress is applied. Giulio Lorenzini et al. [31] investigated the impact of several types of cut-outs on the buckling of the plate and discovered that by selecting the right cut-out method, a high performance might be achieved, i.e., performance could be improved by eliminating a similar quantity of material. Using the Ritz energy equation, Adah et al. [32] develop MATLAB software to determine the critical buckling load for a rectangular plate with an axial compression force. Researchers determined critical buckling coefficients for a variety of boundary conditions and then compared their results to existing literature. By examining the increase in buckling stress caused by cut-outs, Blesa, Gracia, and Rammerstorfer [33] determined that cut-outs can enhance plate buckling strength while decreasing weight. Caio César Cardoso da Silva and colleagues [34] looked into the impact of hexagonal opening geometric arrangements on buckling mechanical characteristics and found that a longitudinally hexagonal cut-out outperforms an oblique hexagonal cut-out. The basic buckling of annular and circular plates with guided edges [12,35] and elastic edges [36,37] was investigated by Rao and Rao. They did not, however, consider the perforation in their research. Using the finite element approach, Sinha et al. [5] performed a buckling study on stainless-steel plates either with or without perforation. The influence of plate length, thickness, and diamond-shape hole-size on buckling load values was investigated. The purpose of Gore and Lokavaraput's research [1] was to explore how material characteristics and geometrical modifications influenced the buckling load bearing capacity of rectangular flat sheets joined on both sides. A comparison was made between a solid plate and a plate with a perforation. Variations in the orientation of the elliptical perforation and the greatest buckling load that could be attained were explored. Fu and Wang [38] devised a new phenomenological galaxy formation model for the critical buckling load of perforated plates with characteristic equations based on the Timoshenko shear beam theory. The suggested model's results were compared to those produced using FEM and found to be in excellent agreement. Using FEM, Hosseinpour et al. [39] investigated the behavior of steel plates with a central circular cut-out when exposed to compressive axial force. As a consequence, an ANN-based formula for determining perforated steel plate's ultimate strength was developed, and its reliability was contrasted to that of previous research formulas.

As stated above, the buckling examination of plates with varied perforation shapes, sizes, orientations, and locations has been the subject of various research. Their findings showed that plate buckling is influenced by perforations' form, size, and direction. Yet, there are several opportunities to investigate the influence of these factors in various combinations [5]. Plates are integral structural members with wide applications in civil engineering, aerospace, and shipbuilding. They are used in construction as it reduces the weight of structures considerably. They are used as the main load-carrying structural member in all these applications. Columns are one-dimensional load-carrying members and plates are two-dimensional load-carrying members used in buildings, bridges, airplanes, and ships. Buckling is the major failure phenomenon observed in plates. Buckling happens when plates are subjected to axial compressive loads. It is important to ensure that plates fail by yielding rather than by buckling. This can be done by keeping the critical buckling stress above yield stress. The support conditions of the plates affect the critical buckling load. The width-thickness ratio of the plates can be adjusted to ensure that buckling stress is above yield stress for different support conditions. Analytical formulas are available for calculating the critical buckling load in plates with different support conditions [40]. Openings or cut-outs are provided in plate elements for increasing the serviceability of the plate structural elements used in structures. The presence of openings always changes the load-carrying capacity and structural stability of plate structures. Openings create a redistribution of stresses and change the buckling behavior. It develops stress concentration

around the openings. Openings reduce the mass of the plates, and it has been found that the presence of openings increases the critical buckling load capacity of plates [41,42].

Analysis of plates with openings is very complex, and due to this complexity, finite element methods (FEM) are usually sought after for such analyses, which are validated using experimental methods. Many FEM and experimental studies have been conducted to study the behavior of plates with openings [43,44]. While experimental studies are destructive and costly, FEM studies are less costly, non-destructive, and less time-consuming. Using the data sets from experimental and FEM studies, the critical buckling load of plates with openings has been calculated using the buckling coefficient method [45] and predicted using various statistical methods [46]. Meanwhile, Wu et al. [47] deployed the differential quadrature method (DQM) to analyze the isotropic and composite laminated plates and shells with particular consideration to the hierarchical finite element method (HFEM). This research utilized the layer-wise theory with linear expansion in each layer to develop a p-version curved laminated composite. It was found that this method used fewer degrees of freedom and less input data to model a complicated case based on interpolation on arc length coordinates. The Bezier method was also used by Kabir et al. [48] for nonlinear vibration and post-buckling of random checkerboard composites reinforced with graphene nano-platelets. This robust Bezier-based solution recommended a probabilistic model to determine a matrix modulus of the graphene nano-platelets reinforced composite.

Artificial intelligence (AI) has many applications to the civil engineering field, specifically in predicting the buckling load of stiffened panels, imperfect reticulates shells, and thin cylindrical shells [49–52]. It can reduce the complexity of practical civil engineering problems to a large extent by making use of already existing experimental studies and results. Civil engineering design practices have moved from their infancy to a state of maturity through the development of design codes. These design codes have been developed based on years of exhaustive experimental studies conducted in relevant areas. AI is one step ahead of these methods due to its capacity to handle large data sets [53,54]. This will bring more accuracy to the results predicted. In this research paper, the critical buckling load of rectangular steel plates with circular cut outs loaded with uniaxial compressive load was predicted with different AI techniques.

2. Materials and Methods

2.1. Steel Setup and Experimental Data Collection

In the present study, a critical buckling load of rectangular steel plates with circular cut-outs loaded with uniaxial compressive load as depicted in Figure 1 was studied.

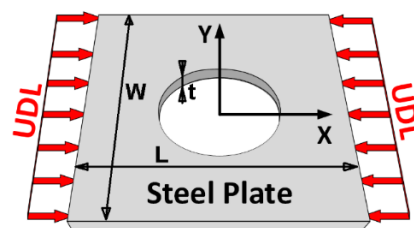


Figure 1. Uniaxial loaded steel plate with a centrally placed circular opening under uniformly distributed loading (UDL).

The support conditions considered are simply supported on all four sides (SSSS), clamped free clamped free (CFCF) and simply supported clamped simply supported clamped (SCSC). Figure 2 depicts the various support conditions.

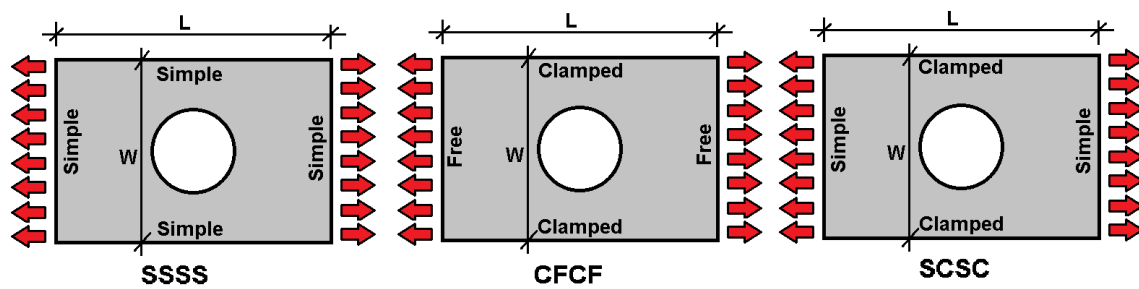


Figure 2. Support conditions of the steel plate.

The independent variables considered are the aspect ratio (length/breadth ratio) of the plate, the thickness of the plate, and the radius of the circular opening, whereas the dependent variable is the buckling load. AI techniques like genetic programming, artificial neural network, and evolutionary polynomial regression have been used to predict the critical buckling loads of steel plates.

2.2. Collected Database and Statistical Analysis

At the end of the loading exercise, 103 experimental test results were collected for rectangular steel plates with centrally placed circular holes with different configurations as presented in the Appendix A to determine their buckling load. Each record contains the following data:

- Aspect ratio (length/width) (L/W),
- Slenderness ratio (width/thickness) (W/t),
- Loss ratio (hole diameter/width) (D/W),
- Boundary conditions (buckling coefficient in width dir. x buckling coef. in length dir.) (Kx.Ky), where K = 2.00 for clamp-free, 1.00 for simple-simple, 0.75 for simple-clamp, and 0.50 for clamp-clamp,
- Relative buckling stress (buckling stress/yielding stress) (Fb/Fy), where buckling stress = buckling load/net area = $\frac{P_b}{(L-D)t}$

The collected records were divided into training (73 records) and validation sets (30 records). The validation set (testing set) was randomly selected and it was the hold-out of the training process and used to test the trained model. Tables 1 and 2 summarized their statistical characteristics and the Pearson correlation matrix. Finally, Figure 3 shows the histograms for both inputs and outputs.

Table 1. Statistical analysis of collected database.

	(L/W)	(W/t)	(D/W)	(Kx.Ky)	(Fb/Fy)
Training set					
Min.	1.00	41.67	0.08	0.50	0.01
Max.	10.00	700.00	0.90	4.00	1.02
Avg	1.80	92.10	0.21	2.51	0.36
SD	1.51	113.76	0.17	1.60	0.32
Var	0.83	1.24	0.82	0.64	0.88
Validation set					
Min.	1.0	20.0	0.1	0.5	0.0
Max.	10.0	500.0	0.6	4.0	1.0
Avg	2.1	90.0	0.2	2.0	0.3
SD	1.8	98.5	0.2	1.6	0.3
Var	0.82	1.09	0.83	0.79	0.91

Table 2. Pearson correlation matrix.

	L/W	W/t	D/W	Kx.Ky	Fb/Fy
L/W	1.00				
W/t	0.04	1.00			
D/W	−0.14	−0.21	1.00		
Kx.Ky	−0.28	−0.44	0.28	1.00	
Fb/Fy	−0.31	−0.27	−0.11	−0.23	1.00

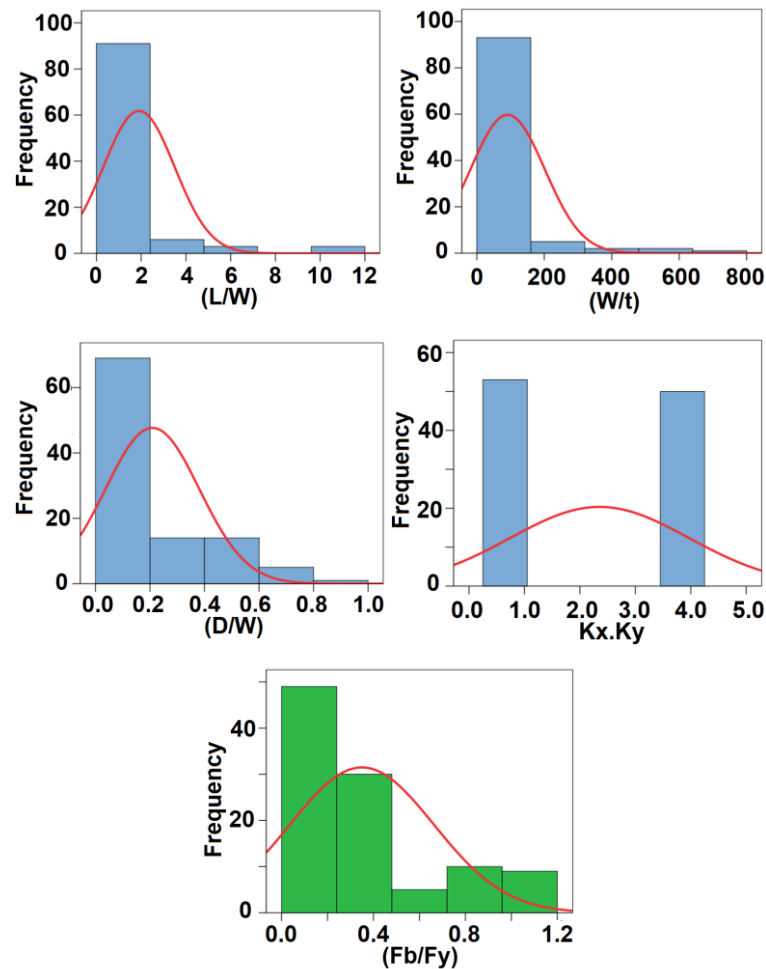


Figure 3. Distribution histograms for inputs (in blue) and outputs (in green).

2.3. Research Program

Three different artificial intelligence (AI) techniques were used to predict the buckling stress of perforated plates or plates with cut outs. These techniques are gene expression programming (GEP), artificial neural network (ANN) and polynomial linear regression optimized using a genetic algorithm which is known as evolutionary polynomial regression (EPR). All three developed models were used to predict the values of relative buckling stress (Fb/Fy) using an aspect ratio (L/W), slenderness ratio (W/t), loss ratio (D/W), and boundary conditions (Kx.Ky). Each model of the three developed models was based on a different approach (evolutionary approach for GEP, mimicking biological neurons for ANN, and optimized mathematical regression technique for EPR). However, for all developed models, prediction accuracy was evaluated in terms of the sum of squared errors (SSE).

The following section discusses the results of each model. The performance accuracies of developed models were evaluated by comparing the (SSE) between predicted and calculated (Fb/Fy) values.

3. Results and Discussion

3.1. Prediction of Relative Buckling Stress (Fb/Fy)

3.1.1. Model (1)—Using GEP Technique

The developed GP model started with 50 gene/chromosomes and settled at 250 gene/chromosomes. The population size, survivor size, and number of generations were 1000, 300, and 200, respectively. Equation (1) presents the output formulas for Fb/Fy. The average error percentage of the total set is 22.7%, while the R² value is 0.932.

$$\frac{F_b}{F_y} = 0.9 \left(\frac{W}{L} \right)^{\exp\left(\frac{W}{CL}\right)} + \left(\frac{\sqrt{W/D}}{K_x.K_y} + \frac{W}{5.6D} \right) \left(\frac{t}{W} \right) \left(1 - \frac{D}{W} \right) \tag{1}$$

where $C = 0.422 \left(\frac{\sqrt{D/W}}{(W/D) - \log(0.42 K_x.K_y)} + 1 \right)$

3.1.2. Model (2)—Using ANN Technique

A GRG-trained ANN with one hidden layer and a HyperTanh activation function was used to predict the same Fb/Fy values. The used network layout of a 4-4-1 ANN model and its connation weights are illustrated in Figure 4 and Table 3. The developed ANN was created and trained using SPSS software. It was sequentially trained with a learning rate of 0.05, the model stopped training when the reduction in errors between two successive epochs was less than 1%. Since ANN has a nonlinear activation function, it cannot be converted into an equivalent equation. The average error percentage of the total dataset for this network is 10.4% and the R² value is 0.986. The relative importance values for each input parameter are illustrated in Figure 5, which indicated that the aspect ratio (L/W) was the most important factor, followed by the sereneness ratio (W/t), while other factors have less influence, which agrees with a previous work [55].

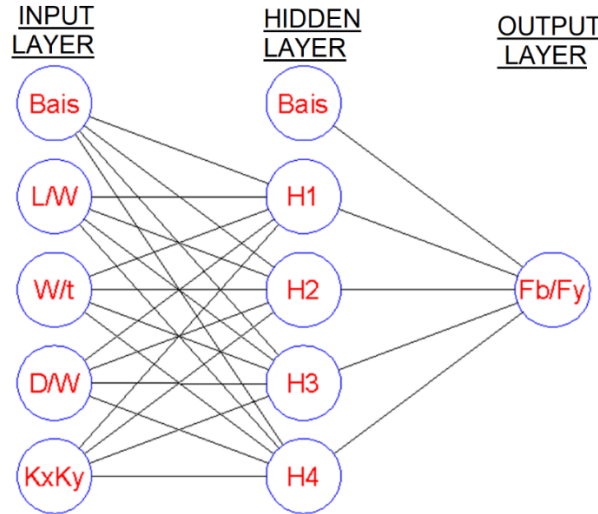


Figure 4. Layout for the developed ANN and its connection weights.

Table 3. Weight matrix for the developed ANN model.

	H1	H2	H3	H4	
(Bias)	13.70	1.37	9.75	8.58	
L/W	10.88	−6.93	2.93	13.16	
W/t	−3.84	3.82	21.04	−3.67	
D/W	−0.63	−0.49	−1.57	0.85	
Kx.Ky	−5.89	7.93	−3.19	−3.07	
	H1	H2	H3	H4	(Bias)
Fb/Fy	−5.23	−10.61	−27.02	−10.32	−22.31

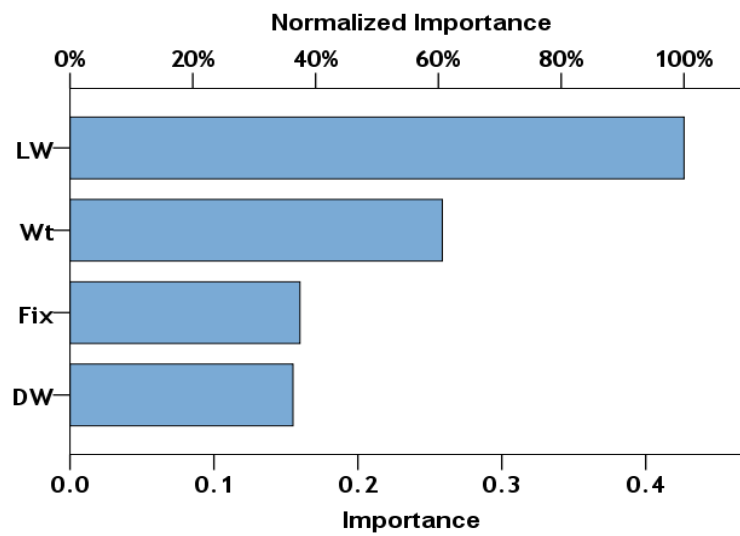


Figure 5. Relative importance of input parameters.

3.1.3. Model (3)—Using EPR Technique

Finally, the developed EPR model was limited to quadrilateral level, for 4 inputs; there are 70 possible terms (35 + 20 + 10 + 4 + 1 = 210) as follows:

$$\sum_{i=1}^{i=4} \sum_{j=1}^{j=4} \sum_{k=1}^{k=4} \sum_{l=1}^{l=4} X_i \cdot X_j \cdot X_k \cdot X_l + \sum_{i=1}^{i=4} \sum_{j=1}^{j=4} \sum_{k=1}^{k=4} X_i \cdot X_j \cdot X_k + \sum_{i=1}^{i=4} \sum_{j=1}^{j=4} X_i \cdot X_j + \sum_{i=1}^{i=4} X_i + C$$

The GA technique was applied to these 70 terms to select the most effective 10 terms to predict the values of Fb/Fy. The outputs are illustrated in Equation (2). The average error percentage and R² values were 15.3% & 0.970 for the total datasets. The results of all developed models are summarized in Table 4.

$$\frac{F_b}{F_y} = \frac{K_x \cdot K_y \cdot L^2}{4165 \cdot W \cdot D} + \frac{K_x \cdot K_y \cdot W \cdot D + 53540 \cdot t^2}{605 \cdot L \cdot t} + \frac{1.7W(2.1K_x \cdot K_y - 1)}{L(K_x \cdot K_y)^3} - \left(\frac{W}{L}\right)^2 \left(\frac{30760 \cdot t + W}{41565 \cdot t}\right) + \frac{28.9 \cdot t[1 - (2 \cdot K_x \cdot K_y)^2]}{W(K_x \cdot K_y)^3} - 0.25 \tag{2}$$

Table 4. Accuracies of developed models.

Technique	Developed Eq.	SSE	Error %	R ²
GEP	Equation (1)	0.65	22.7	0.932
ANN	Figure 2	0.14	10.4	0.986
EPR	Equation (2)	0.30	15.3	0.970

The relations between calculated and predicted values for all developed models are shown in Figure 6.

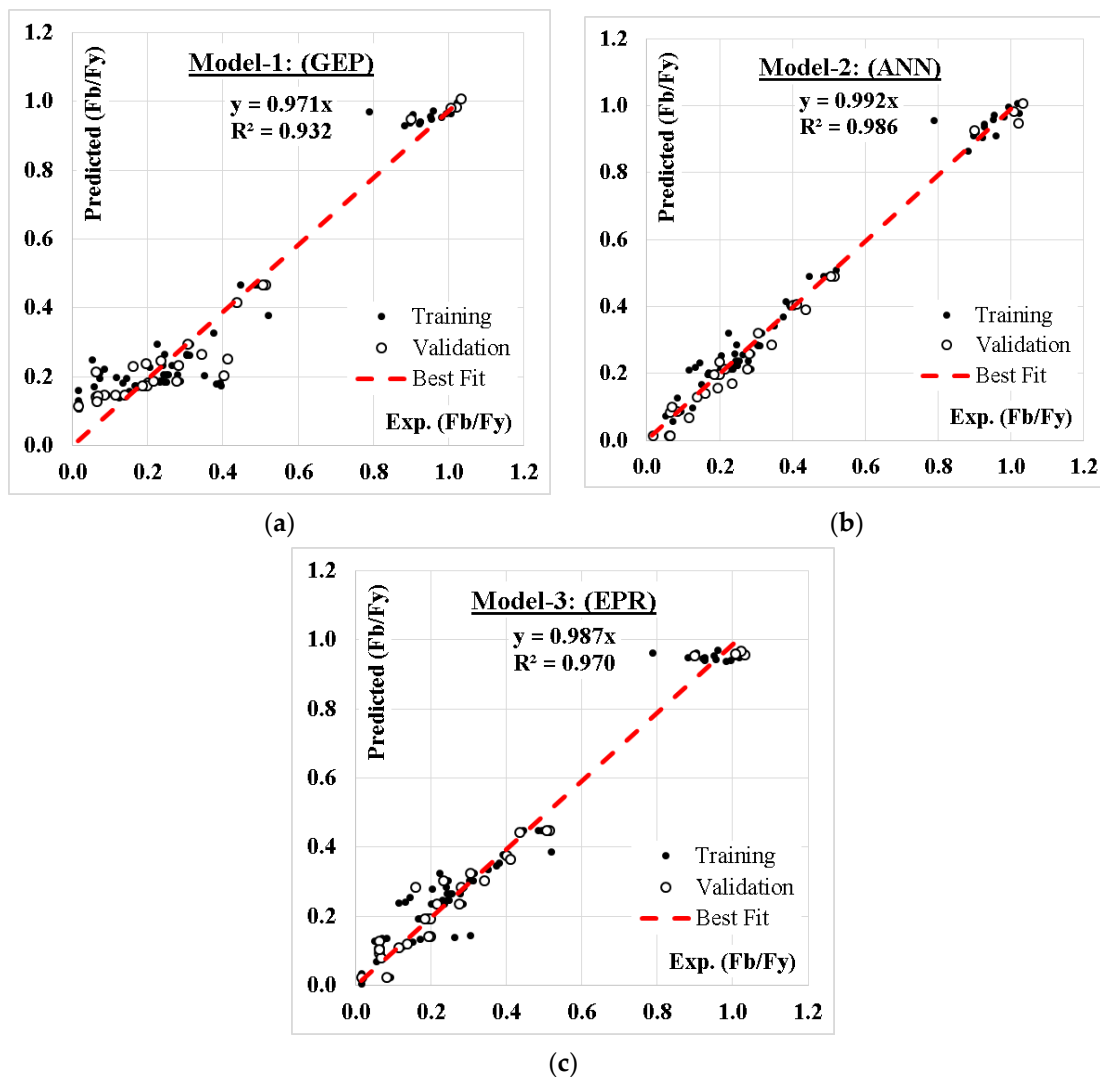


Figure 6. Relation between predicted and calculated Fb/Fy values using the developed models. (a) using GEP, (b) using ANN & (c) using EPR.

4. Conclusions

This research presented three models using three AI techniques (GEP, ANN and EPR) to predict the values of relative buckling stress (Fb/Fy) using an aspect ratio (L/W), slenderness ratio (W/t), loss ratio (D/W), and boundary conditions (Kx.Ky). The results of comparing the accuracies of the developed models can be concluded in the following points:

- Both ANN and EPR have the most similar prediction accuracy, 89.6% and 84.7%, respectively, while the GEP model has the lowest prediction accuracy (77.3%).
- Although, the error percentage of the ANN and EPR models were so close, the output of the EPR model was closed form equations which could be manually used or as software unlike the ANN output which cannot be manually used.
- The summation of the absolute weights of each neuron in the input layer of the developed (ANN) model indicated that aspect ratio (L/W) had major influences on the relative buckling stress rather than the slenderness ratio (W/t), while the loss ratio (D/W) and boundary conditions (Kx.Ky) had less impact on (Fb/Fy).
- The GA technique successfully reduced the 70 terms of conventional polynomial regression quadrilateral formula to only 10 terms without significant impact on its accuracy.

- Like any other regression technique, the generated formulas were valid within the considered range of parameter values, beyond this range the prediction accuracy should be verified.

Author Contributions: Conceptualization, K.C.O.; methodology, A.M.E.; formal analysis, A.S.; investigation, M.D.; data curation, J.J.; supervision, H.J. All authors have read and agreed to the published version of the manuscript.

Funding: This research received no external funding.

Institutional Review Board Statement: Not applicable.

Informed Consent Statement: Not applicable.

Data Availability Statement: Utilized data are available in the Appendix A.

Conflicts of Interest: The authors declare no conflict of interest.

Appendix A. Utilized Database

L/W.	W/t.	D/W.	Kx.Ky	Fb/Fy.	L/W.	W/t.	D/W.	Kx.Ky	Fb/Fy.
1.5.	48.	0.20.	4.0.	0.25.	1.5.	48.	0.35.	1.0.	0.08.
1.5.	48.	0.50.	4.0.	0.25.	1.5.	48.	0.20.	4.0.	0.25.
1.5.	48.	0.40.	4.0.	0.24.	5.0.	200.	0.10.	0.5.	0.02.
1.0.	63.	0.08.	1.0.	1.02.	1.5.	48.	0.10.	4.0.	0.23.
1.5.	48.	0.10.	4.0.	0.29.	1.7.	600.	0.10.	0.5.	0.02.
1.5.	48.	0.40.	4.0.	0.26.	1.5.	48.	0.30.	4.0.	0.28.
1.5.	48.	0.25.	1.0.	0.07.	1.5.	48.	0.50.	4.0.	0.30.
1.0.	83.	0.11.	1.0.	0.95.	1.5.	48.	0.70.	4.0.	0.37.
1.5.	48.	0.50.	4.0.	0.30.	1.5.	48.	0.10.	4.0.	0.24.
1.0.	50.	0.16.	1.0.	0.90.	1.0.	42.	0.16.	1.0.	0.96.
1.6.	48.	0.10.	4.0.	0.17.	2.5.	400.	0.10.	0.5.	0.02.
1.0.	63.	0.14.	1.0.	0.95.	2.0.	100.	0.50.	1.0.	0.17.
1.1.	48.	0.10.	4.0.	0.45.	10.0.	50.	0.10.	0.5.	0.07.
1.5.	48.	0.30.	4.0.	0.24.	1.5.	48.	0.30.	4.0.	0.25.
1.0.	63.	0.11.	1.0.	1.01.	1.5.	48.	0.15.	4.0.	0.13.
2.5.	80.	0.10.	0.5.	0.39.	1.5.	48.	0.08.	1.0.	0.05.
1.5.	48.	0.30.	4.0.	0.26.	3.3.	300.	0.10.	0.5.	0.02.
1.5.	48.	0.50.	4.0.	0.31.	1.5.	48.	0.10.	4.0.	0.20.
1.0.	50.	0.14.	1.0.	0.79.	1.4.	700.	0.10.	0.5.	0.01.
2.0.	100.	0.10.	0.5.	0.39.	10.0.	100.	0.10.	0.5.	0.02.
1.0.	83.	0.14.	1.0.	0.93.	1.5.	48.	0.60.	4.0.	0.22.
1.1.	48.	0.10.	4.0.	0.49.	2.0.	100.	0.60.	1.0.	0.20.
1.0.	100.	0.08.	1.0.	0.98.	1.1.	48.	0.10.	4.0.	0.51.
1.7.	120.	0.10.	0.5.	0.38.	2.0.	100.	0.30.	1.0.	0.14.
2.0.	100.	0.40.	1.0.	0.15.	1.5.	48.	0.10.	4.0.	0.28.
1.5.	48.	0.10.	4.0.	0.23.	1.5.	48.	0.50.	4.0.	0.34.
1.5.	48.	0.20.	4.0.	0.23.	2.0.	250.	0.10.	0.5.	0.06.
1.0.	83.	0.08.	1.0.	0.99.	1.1.	48.	0.10.	4.0.	0.51.
2.1.	48.	0.10.	4.0.	0.09.	2.0.	100.	0.10.	1.0.	0.11.
2.1.	48.	0.10.	4.0.	0.09.	1.5.	48.	0.40.	4.0.	0.28.
2.1.	48.	0.10.	4.0.	0.09.	3.3.	60.	0.10.	0.5.	0.40.
1.0.	83.	0.16.	1.0.	0.90.	1.5.	48.	0.40.	1.0.	0.16.
1.5.	48.	0.08.	4.0.	0.12.	2.1.	48.	0.10.	4.0.	0.08.
1.4.	350.	0.10.	0.5.	0.06.	1.0.	50.	0.08.	1.0.	1.03.
3.3.	150.	0.10.	0.5.	0.07.	2.0.	500.	0.10.	0.5.	0.02.
1.5.	48.	0.40.	4.0.	0.29.	10.0.	20.	0.10.	0.5.	0.44.
1.5.	48.	0.60.	4.0.	0.31.	1.6.	48.	0.10.	4.0.	0.19.
1.0.	100.	0.11.	1.0.	0.93.	1.7.	300.	0.10.	0.5.	0.06.
2.1.	48.	0.10.	4.0.	0.09.	1.0.	63.	0.16.	1.0.	0.90.

L/W.	W/t.	D/W.	Kx.Ky	Fb/Fy.	L/W.	W/t.	D/W.	Kx.Ky	Fb/Fy.
1.4.	140.	0.10.	0.5.	0.35.	1.6.	48.	0.10.	4.0.	0.20.
1.0.	42.	0.11.	1.0.	1.02.	1.5.	48.	0.15.	1.0.	0.06.
1.5.	48.	0.10.	4.0.	0.22.	1.5.	48.	0.60.	4.0.	0.31.
1.6.	48.	0.10.	4.0.	0.17.	1.5.	48.	0.45.	1.0.	0.20.
1.5.	48.	0.20.	4.0.	0.25.	1.5.	48.	0.50.	1.0.	0.23.
2.0.	100.	0.20.	1.0.	0.12.	1.5.	48.	0.10.	4.0.	0.22.
1.5.	48.	0.25.	4.0.	0.14.	5.0.	100.	0.10.	0.5.	0.07.
1.5.	48.	0.90.	4.0.	0.52.	1.0.	42.	0.14.	1.0.	1.02.
1.5.	48.	0.10.	4.0.	0.21.	2.5.	200.	0.10.	0.5.	0.06.
1.0.	100.	0.14.	1.0.	0.92.	1.0.	50.	0.11.	1.0.	1.01.
1.1.	48.	0.10.	4.0.	0.49.	1.6.	48.	0.10.	4.0.	0.19.
1.5.	48.	0.38.	4.0.	0.21.	5.0.	40.	0.10.	0.5.	0.41.
1.0.	100.	0.16.	1.0.	0.88.

References

- Gore, R.; Lokavarapu, B.R. Effect of Elliptical Cutout on Buckling Load for Isotropic Thin Plate. In *Innovations in Mechanical Engineering*; Narasimham, G.S.V.L., Babu, A.V., Reddy, S.S., Dhanasekaran, R., Eds.; Springer: Singapore, 2022; pp. 51–69.
- Al Qablan, H. Applicable Formulas for Shear and Thermal Buckling of Perforated Rectangular Panels. *Adv. Civ. Eng.* **2022**, *2022*, 3790462. [[CrossRef](#)]
- Dehadray, P.M.; Alampally, S.; Lokavarapu, B.R. Buckling Analysis of Thin Isotropic Square Plate with Rectangular Cut-Out. In *Innovations in Mechanical Engineering*; Narasimham, G.S.V.L., Babu, A.V., Reddy, S.S., Dhanasekaran, R., Eds.; Springer: Singapore, 2022; pp. 71–86.
- Taherian, I.; Ghalehnovi, M.; Jahangir, H. Analytical Study on Composite Steel Plate Walls Using a Modified Strip Model. In *Proceedings of the 10th International Congress on Civil Engineering*, Abriz, Iran, 5–7 May 2015.
- Sinha, V.; Patel, R.; Ghetiya, K.; Nair, M.; Trivedi, T.; Rao, L.B. Impact of Diamond-Shaped Cut-Out on Buckling Nature of Isotropic Stainless-Steel Plate. In *Innovations in Mechanical Engineering*; Narasimham, G.S.V.L., Babu, A.V., Reddy, S.S., Dhanasekaran, R., Eds.; Springer: Singapore, 2022; pp. 119–146.
- Soleymani, A.; Reza Esfahani, m. Effect of concrete strength and thickness of flat slab on preventing of progressive collapse caused by elimination of an internal column. *J. Struct. Constr. Eng.* **2019**, *6*, 24–40. [[CrossRef](#)]
- Hosseini-Hashemi, S.; Khorshidi, K.; Amabili, M. Exact solution for linear buckling of rectangular Mindlin plates. *J. Sound Vib.* **2008**, *315*, 318–342. [[CrossRef](#)]
- Orun, A.E.; Guler, M.A. Effect of hole reinforcement on the buckling behaviour of thin-walled beams subjected to combined loading. *Thin-Walled Struct.* **2017**, *118*, 12–22. [[CrossRef](#)]
- Singh, T.G.; Chan, T.-M. Effect of access openings on the buckling performance of square hollow section module stub columns. *J. Constr. Steel Res.* **2021**, *177*, 106438. [[CrossRef](#)]
- Hasrati, E.; Ansari, R.; Rouhi, H. A numerical approach to the elastic/plastic axisymmetric buckling analysis of circular and annular plates resting on elastic foundation. *Proc. Inst. Mech. Eng. Part C J. Mech. Eng. Sci.* **2019**, *233*, 7041–7061. [[CrossRef](#)]
- Russell, M.J.; Lim, J.B.; Roy, K.; Clifton, G.C.; Ingham, J.M. Welded steel beam with novel cross-section and web openings subject to concentrated flange loading. *Structures* **2020**, *24*, 580–599. [[CrossRef](#)]
- Rao, L.B.; Rao, C.K. Buckling of Circular Plates with an Internal Elastic Ring Support and Elastically Restrained Guided Edge Against Translation. *Mech. Based Des. Struct. Mach.* **2009**, *37*, 60–72. [[CrossRef](#)]
- Jahangir, H.; Daneshvar Khorram, M.H.; Ghalehnovi, M. Influence of geometric parameters on perforated core buckling restrained braces behavior. *J. Struct. Constr. Eng.* **2019**, *6*, 75–94. [[CrossRef](#)]
- Daneshvar, M.H.; Saffarian, M.; Jahangir, H.; Sarmadi, H. Damage identification of structural systems by modal strain energy and an optimization-based iterative regularization method. *Eng. Comput.* **2022**, *37*, 1–21. [[CrossRef](#)]
- Jahangir, H.; Khatibinia, M.; Kavousi, M. Application of Contourlet Transform in Damage Localization and Severity Assessment of Prestressed Concrete Slabs. *Soft Comput. Civ. Eng.* **2021**, *5*, 39–67. [[CrossRef](#)]
- Muddappa, P.P.Y.; Rajanna, T.; Giridhara, G. Effect of reinforced cutouts on the buckling and vibration performance of hybrid fiber metal laminates. *Mech. Based Des. Struct. Mach.* **2021**, *49*, 1–21. [[CrossRef](#)]
- Mohammadzadeh, B.; Choi, E.; Kim, W.J. Comprehensive investigation of buckling behavior of plates consider-ing effects of holes. *Struct. Eng. Mech.* **2018**, *68*, 261–275. [[CrossRef](#)]
- Abolghasemi, S.; Eipakchi, H.; Shariati, M. An analytical solution for buckling of plates with circular cutout subjected to non-uniform in-plane loading. *Arch. Appl. Mech. Vol.* **2019**, *89*, 2519–2543. [[CrossRef](#)]
- Kim, J.-H.; Park, D.-H.; Kim, S.-K.; Kim, J.-D.; Lee, J.-M. Lateral Deflection Behavior of Perforated Steel Plates: Experimental and Numerical Approaches. *J. Mar. Sci. Eng.* **2021**, *9*, 498. [[CrossRef](#)]
- Yidris, N.; Hassan, M. The effects of cut-out on thin-walled plates. In *Modelling of Damage Processes in Biocomposites, Fibre-Reinforced Composites and Hybrid Composites*; Woodhead Publishing: Philadelphia, PA, USA, 2019. [[CrossRef](#)]

21. Kumar, M.S.; Alagusundaramoorthy, P.; Sundaravadivelu, R. Ultimate strength of square plate with rectangular opening under axial compression. *J. Nav. Arch. Mar. Eng.* **2007**, *4*, 15–26. [[CrossRef](#)]
22. Maiorana, E.; Pellegrino, C.; Modena, C. Linear buckling analysis of perforated plates subjected to localised symmetrical load. *Eng. Struct.* **2008**, *30*, 3151–3158. [[CrossRef](#)]
23. Singh, S.; Kulkarni, K.; Pandey, R.; Singh, H. Buckling analysis of thin rectangular plates with cutouts subjected to partial edge compression using FEM. *J. Eng. Des. Technol.* **2012**, *10*, 128–142. [[CrossRef](#)]
24. Shariati, M.; Dadrasi, A. Numerical and Experimental Investigation of Loading Band on Buckling of Perforated Rectangular Steel Plates. *Res. J. Recent Sci.* **2012**, *1*, 63–71.
25. Djelosevic, M.; Tepic, J.; Tanackov, I.; Kostelac, M. Mathematical Identification of Influential Parameters on the Elastic Buckling of Variable Geometry Plate. *Sci. World J.* **2013**, *2013*, 268673. [[CrossRef](#)]
26. De Mauro Vasconcellos, R.; Liécio André, I.; Alexandra Pinto, D.; Daniel, H. Elastic and Elasto-Plastic Buckling Analysis of Perforated Steel Plates. Repositório Inst. 2013. Available online: <https://repositorio.furg.br/handle/1/4929> (accessed on 1 May 2022).
27. Behzad, M.; Noh, H.-C. Use of Buckling Coefficient in Predicting Buckling Load of Plates with and without Holes. *J. Korean Soc. Adv. Compos. Struct.* **2014**, *5*, 1–7. [[CrossRef](#)]
28. Mohammadzadeh, B.; Noh, H.C. Investigation into the buckling coefficients of plates with holes considering variation of hole size and plate thickness. *Mechanika* **2016**, *22*, 167–175. [[CrossRef](#)]
29. Shariati, M.; Faradjian, Y.; Mehrabi, H. Numerical and Experimental Study of Buckling of Rectangular Steel Plates with a Cutout. *J. Solid Mech.* **2016**, *8*, 116–129.
30. Jana, P. Optimal design of uniaxially compressed perforated rectangular plate for maximum buckling load. *Thin-Walled Struct.* **2016**, *103*, 225–230. [[CrossRef](#)]
31. Lorenzini, G.; Helbig, D.; Silva, C.; Real, M.; Santos, E.; Rocha, L. Numerical evaluation of the effect of type and shape of perforations on the buckling of thin steel plates by means of the constructal design method. *Int. J. Heat Technol.* **2016**, *34*, S9–S20. [[CrossRef](#)]
32. Adah, D.E.; Onwuka, O.M. Ibearugbulem, Matlab Based Buckling Analysis of Thin Rectangular Flat Plates. *Am. J. Eng. Res.* **2019**, *8*, 224–228.
33. Gracia, J.B.; Rammerstorfer, F.G. Increase in buckling loads of plates by introduction of cutouts. *Acta Mech.* **2019**, *230*, 2873–2889. [[CrossRef](#)]
34. Da Silva, C.C.C.; Helbig, D.; Cunha, M.L.; dos Santos, E.D.; Rocha, L.A.O.; Real, M.D.V.; Isoldi, L.A. Numerical buckling analysis of thin steel plates with centered hexagonal perforation through constructal design method. *J. Braz. Soc. Mech. Sci. Eng.* **2019**, *41*, 309. [[CrossRef](#)]
35. Rao, L.B.; Rao, C.K. Fundamental Buckling of Annular Plates with Elastically Restrained Guided Edges Against Translation. *Mech. Based Des. Struct. Mach.* **2011**, *39*, 409–419. [[CrossRef](#)]
36. Rao, L.B.; Rao, C.K. Buckling of circular plate with foundation and elastic edge. *Int. J. Mech. Mater. Des.* **2015**, *11*, 149–156. [[CrossRef](#)]
37. Rao, L.B.; Rao, C.K. Buckling of Annular Plates with Elastically Restrained External and Internal Edges. *Mech. Based Des. Struct. Mach.* **2013**, *41*, 222–235. [[CrossRef](#)]
38. Fu, W.; Wang, B. A semi-analytical model on the critical buckling load of perforated plates with opposite free edges. *Proc. Inst. Mech. Eng. Part C J. Mech. Eng. Sci.* **2022**, *236*, 4885–4894. [[CrossRef](#)]
39. Hosseinpour, P.; Hosseinpour, M.; Sharifi, Y. Artificial neural networks for predicting ultimate strength of steel plates with a single circular opening under axial compression. *Ships Offshore Struct.* **2022**, *17*, 1–16. [[CrossRef](#)]
40. Timoshenko, S.P.; Gere, J.M. *Theory of Elastic Stability*; Tata McGraw-Hill Education Pvt. Ltd.: New Delhi, India, 2010.
41. Ebid, A.M.; El-Aghoury, M.A.; Onyelowe, K.C. Estimating the Optimum Weight for Latticed Power-Transmission Towers Using Different (AI) Techniques. *Designs* **2022**, *6*, 62. [[CrossRef](#)]
42. Reda, M.A.; Ebid, A.M.; Ibrahim, S.M.; El-Aghoury, M.A. Strength of Composite Columns Consists of Welded Double CF Sigma-Sections Filled with Concrete—An Experimental Study. *Designs* **2022**, *6*, 82. [[CrossRef](#)]
43. Nemeth, M.P. Buckling behavior of compression-loaded symmetrically laminated angle-ply plates with holes. *AIAA J.* **1988**, *26*, 330–336. [[CrossRef](#)]
44. Faradjian Mohtaram, Y.; Taheri Kahnamouei, J.; Shariati, M.; Behjat, B. Experimental and numerical investigation of buckling in rectangular steel plates with groove-shaped cutouts. *J. Zhejiang Univ. Sci. A* **2012**, *13*, 469–480. [[CrossRef](#)]
45. Kelpša, Š.; Peltonen, S. Local Buckling Coefficient Calculation Method of Thin Plates with Round Holes. *ce/Papers* **2019**, *3*, 841–846. [[CrossRef](#)]
46. Shi, J.; Guo, L.; Gao, S. Study on the buckling behavior of steel plate composite walls with diamond ar-ranged studs under axial compression. *J. Build. Eng.* **2022**, *50*, 2352–7102.
47. Wu, Y.; Xing, Y.; Liu, B. Analysis of isotropic and composite laminated plates and shells using a differential quadrature hierarchical finite element method. *Compos. Struct.* **2018**, *205*, 11–25. [[CrossRef](#)]
48. Kabir, H.; Aghdam, M. A robust Bézier based solution for nonlinear vibration and post-buckling of random checkerboard graphene nano-platelets reinforced composite beams. *Compos. Struct.* **2019**, *212*, 184–198. [[CrossRef](#)]

49. Sun, Z.; Lei, Z.; Bai, R.; Jiang, H.; Zou, J.; Ma, Y.; Yan, C. Prediction of compression buckling load and buckling mode of hat-stiffened panels using artificial neural network. *Eng. Struct.* **2021**, *242*, 112275. [[CrossRef](#)]
50. Zhu, S.; Ohsaki, M.; Guo, X. Prediction of non-linear buckling load of imperfect reticulated shell using modified consistent imperfection and machine learning. *Eng. Struct.* **2020**, *226*, 111374. [[CrossRef](#)]
51. Badarloo, B.; Jafari, F. A Numerical Study on the Effect of Position and Number of Openings on the Performance of Composite Steel Shear Walls. *Buildings* **2018**, *8*, 121. [[CrossRef](#)]
52. Tahir, Z.U.R.; Mandal, P.; Adil, M.T.; Naz, F. Application of artificial neural network to predict buckling load of thin cylindrical shells under axial compression. *Eng. Struct.* **2021**, *248*, 113221. [[CrossRef](#)]
53. Abambres, M.; Rajana, K.; Tsavdaridis, K.D.; Ribeiro, T.P. Neural Network-Based Formula for the Buckling Load Prediction of I-Section Cellular Steel Beams. *Computers* **2018**, *8*, 2. [[CrossRef](#)]
54. El-Aghoury, M.A.; Ebid, A.M.; Onyelowe, K.C. Optimum Design of Fully Composite, Unstiffened, Built-Up, Hybrid Steel Girder Using GRG, NLR, and ANN Techniques. *J. Eng.* **2022**, *2022*, 7439828. [[CrossRef](#)]
55. Kadry, A.A.; Ebid, A.M.; Mokhtar, A.-S.A.; El-Ganzoury, E.N.; Haggag, S.A. Parametric study of Unstiffened multi-planar tubular KK-Joints. *Results Eng.* **2022**, *14*, 100400. [[CrossRef](#)]